Smith predictor-based feedforward controller for measurable disturbances

René D.O. Pereira, Bismark C. Torrico, José N. Do Nascimento Jr., Thiago Alves Lima, Magno P. de Almeida Filho, Fabrício G Nogueira

Smith predictor-based feedforward controller for measurable disturbances

René D. O. Pereira[a,*], Bismark C. Torrico[a], José N. do Nascimento Jr.[a], Thiago Alves Lima[b], Magno P. de Almeida Filho[c], Fabrício G. Nogueira[a]

[a] *Department of Electrical Engineering, Federal University of Ceara, 60455-760, Fortaleza-CE, Brazil*
[b] *Université de Lorraine, CNRS, CRAN, Nancy F-54000, France*
[c] *Federal Institute of Education, Science and Technology of Ceara, Boa Viagem-CE, Brazil*

Abstract

This paper proposes a feedforward extension for the simplified filtered Smith predictor (SFSP) to deal with measurable disturbances. The proposed strategy uses a state-space formulation and can be applied in unified manner to stable, unstable, and integrating linear dead-time processes of any order. The main advantage with using the predictor approach in comparison with other control strategies is the ability to deal with processes with large dead time. The structure improves the disturbance rejection performance by feedforwarding the disturbance while maintaining the good robustness and noise attenuation properties of the SFSP. Simulation results show better performance indices compared with other strategies from the recent literature. In addition, the proposed strategy is applied to control the temperature in a newborn intensive care unit (NICU) to show its effectiveness in a real process.

Keywords: Smith predictor, feedforward control, dead-time compensator, measurable disturbances, newborn intensive care unit.

1. Introduction

In process control, disturbance rejection is a theme of great relevance (Albertos et al., 2015). In the industry, a control system with good disturbance rejection leads to improvements in several aspects, ranging from process operation safety to economical advantages. Moreover, it is directly related to the quality of final products, decrease in production costs, energy saving, etc.

In the case of measurable disturbances, its rejection can be significantly improved by feedforwarding its values in the control signal before the disturbance affects the process output. Many works in the past years have studied this control problem (Davison,

*Corresponding author
Email addresses: reneolimpio@alu.ufc.br (René D. O. Pereira), bismark@dee.ufc.br (Bismark C. Torrico), juniornogueira@alu.ufc.br (José N. do Nascimento Jr.), thiago.alves-lima@univ-lorraine.fr (Thiago Alves Lima), magno.prudencio@ifce.edu.br (Magno P. de Almeida Filho), fnogueira@dee.ufc.br (Fabrício G. Nogueira)

1973; Guzmán and Hägglund, 2011; Hast and Hägglund, 2014; Silva et al., 2018), but only a few deal with the presence of dead time in the process (Rodríguez et al., 2016; Rodríguez et al., 2016; Alves Lima et al., 2019; Sanz et al., 2021; Rodríguez et al., 2020; García-Mañas et al., 2021).

Dead times are present in several industrial processes and can cause performance deterioration or even instability of the closed loop when regulated by traditional controllers, such as proportional-integral-derivative (PID), due to the phase margin being affected by the time delay. One of the first and most widespread solutions to compensate dead time was proposed in Smith (1957). This solution is valid for open-loop stable processes, which was later known as the Smith predictor (SP) because the output of the delay-free model is predicted to compensate the dead time. Since then, many authors have studied the SP properties and drawbacks.

One of the most important modifications was the filtered Smith predictor (FSP), whose main idea is to include a filter in the prediction structure to (i) improve the robustness properties of the closed-loop, (ii) reject different kinds of disturbances, like steps, ramps, and sinusoidal, and (iii) guarantee robust stability for open-loop integrating and unstable processes (Normey-Rico and Camacho, 2007, 2009). Many other controllers based on predictors and extended observers for time-delay systems can be found in the literature (Castillo et al., 2019; Sanz et al., 2020; Castillo and García, 2021).

In the works García and Albertos (2013); Liu et al. (2018); Sanz et al. (2018), the authors have proposed control structures based on a stable predictor, also denoted as Generalized predictor (GP) (Albertos and García, 2009). The results were generalized for stable, integrating, and unstable open-loop processes.

Many works have also recently emerged to compensate dead times using structures based on active disturbance rejection control (ADRC) (Zhao and Gao, 2014; Liu et al., 2019; Geng et al., 2019; Zhang et al., 2020). The essence of the ADRC is to use an extended state observer to compensate the effect of disturbances and uncertainties. The ADRC-based structures can be applied to open-loop stable, unstable, and integrative time-delayed systems.

Recently, focusing on industrial applications, the works in Torrico et al. (2018, 2021); Sá Rodrigues et al. (2021) have presented simple tuning rules for the FSP, namely SFSP, by using a similar structure of the FSP but with fewer parameters to tune. As a result, the SFSP allowed obtaining better or equivalent results than other structures based on predictors with respect to disturbance rejection and noise attenuation.

For measurable disturbances, feedforward control structures allow attenuating the disturbance effect before it is felt in the process output. This phenomenon also occurs if dead-time compensators are used in the case of time-delay processes. In these kinds of processes, feedforward control structures allow improving the disturbance attenuation even more because the effect of the disturbance is felt in the output only after the disturbance model delay. Most of the aforementioned works do not deal with measurable disturbances for dead-time processes. The work in Rodríguez et al. (2016) proposes a feedforward compensator for the FSP with measurable disturbances. The structure adds a feedforward path, including the disturbance model and a filter used as a tuning parameter. In Alves Lima et al. (2019), the same feedforward structure from

Rodríguez et al. (2016) was applied to the SFSP for first-order dead-time processes, obtaining better disturbance rejection with a lower-order robustness filter. The work in Rodríguez et al. (2020) proposes tuning rules for a feedforward control methodology that uses low-order process models. In García-Mañas et al. (2021), a comparison of recently published tuning rules for feedforward compensation is made by simulations and experiments.

In order to further improve the disturbance rejection in processes with measurable disturbances, this paper proposes a new feedforward structure for the SFSP for high-order dead-time processes. The main novelty comes from the idea of including a static gain in the feedforward path so that the control action can deal in advance with the disturbance prior to its effects on the measured plant output. Furthermore, the proposed controller has the same tuning degrees of freedom as the original SFSP since there are no free tuning parameters to design the feedforward controller. Therefore, the proposed controller has only two tuning parameters, while the predictor-based controllers proposed in Rodríguez et al. (2016); Alves Lima et al. (2019) have three tuning parameters.

The manuscript is organised as follows: Section 2 defines the process model; Section 3 describes the formulation of the SFSP with feedforward action; a guide on how the controller is designed is presented in Section 4; Section 5 presents the stable implementation of the controller; in Section 6 the closed-loop robust stability is analysed; guidelines for tuning the proposed controller are given in Section 7; the simulation examples are presented in Section 8; Section 9 presents experimental results obtained with internal temperature control of a NICU; the final considerations and discussions of the results are shown in Section 10.

2. The process model

Consider a dead-time process where the control input, the measurable disturbance, the output, and the measurement noise are represented, respectively, by u, q, y, $w \in \mathbb{R}$. The Laplace transforms of these signals are, respectively, $U(s)$, $Q(s)$, $Y(s)$, $W(s)$, and their z-transforms are, respectively, $U(z)$, $Q(z)$, $Y(z)$, $W(z)$. Thus, this open-loop process is represented in state space as:

$$\begin{cases} \tilde{x}(t+1) = \tilde{A}\tilde{x}(t) + \tilde{B}\begin{bmatrix} u(t-d) \\ q(t-d_q) \end{bmatrix}, \\ y(t) = \tilde{C}\tilde{x}(t) + w(t), \end{cases} \tag{1}$$

where t is the discrete-time, d and d_q are dead times, $\tilde{x} \in \mathbb{R}^{\tilde{n}}$ are the states, the pair $(\tilde{A}, \tilde{B})$ is controllable, the pair $(\tilde{C}, \tilde{A})$ is observable and $(\tilde{A}, \tilde{B}, \tilde{C})$ are matrices of appropriate dimensions.

For control design, the input-output transfer functions from (1) are computed, whose minimal realisations are given by

$$P(z) = \frac{Y(z)}{U(z)} = G(z)z^{-d} = C(zI - A)^{-1}Bz^{-d} = \mathbb{M}\left[\tilde{C}(zI - \tilde{A})^{-1}\tilde{B}_1\right]z^{-d}, \tag{2}$$

$$P_q(z) = \frac{Y(z)}{Q(z)} = G_q(z)z^{-d_q} = C_q(zI - A_q)^{-1}B_qz^{-d_q} = \mathbb{M}\left[\tilde{C}(zI - \tilde{A})^{-1}\tilde{B}_2\right]z^{-d_q}, \tag{3}$$

where the operator $\mathbb{M}[\cdot]$ is the minimal realisation of $[\cdot]$, $\tilde{B} = [\tilde{B}_1 \ \tilde{B}_2]$, the pairs (A, B) and (A_q, B_q) are controllable, (A, C) and (A_q, C_q) are observable, and the matrices (A, B, C) and (A_q, B_q, C_q) are in the observable canonical form, as shown in Appendix A. In addition, to avoid unstable modes outside the feedback path, it is assumed that the set of eigenvalues λ_i of A_q satisfying the condition $|\lambda_i| \geq 1$ also belongs to the set of eigenvalues of A.

For simulation purposes, the following transfer functions in the s-domain represent the input-output relationships of the open-loop process:

$$P(s) = \frac{Y(s)}{U(s)} = G(s)e^{-Ls} = C^*(sI - A^*)^{-1}B^*e^{-Ls}, \tag{4}$$

$$P_q(s) = \frac{Y(s)}{Q(s)} = G_q(s)e^{-L_q s} = C_q^*(sI - A_q^*)^{-1}B_q^*e^{-L_q s}, \tag{5}$$

where the order of $G(s)$ is n, the order of $G_q(s)$ is n_q, L and L_q are dead times. The pairs (A^*, B^*) and (A_q^*, B_q^*) are controllable, (A^*, C^*) and (A_q^*, C_q^*) are observable, therefore, the state-space representations $(A^*, B^*, C^*, 0)$ and $(A_q^*, B_q^*, C_q^*, 0)$ are, respectively, minimal realisations of $G(s)$ and $G_q(s)$ (Chen, 1984).

By using transfer functions (4) and (5), an augmented state-space process model is given by

$$\begin{cases} \dot{\bar{x}}(t) = \bar{A}\bar{x}(t) + \bar{B}\begin{bmatrix} u(t-L) \\ q(t-L_q) \end{bmatrix}, \\ y(t) = \bar{C}\bar{x}(t) + w(t), \end{cases} \tag{6}$$

where t is the discrete-time, $\bar{x} \in \mathbb{R}^{(n+n_q)}$ are the states,

$$\bar{A} = \begin{bmatrix} A^* & \mathbf{0} \\ \mathbf{0} & A_q^* \end{bmatrix}, \bar{B} = \begin{bmatrix} B^* & \mathbf{0} \\ \mathbf{0} & B_q^* \end{bmatrix}, \bar{C} = \begin{bmatrix} C^* & C_q^* \end{bmatrix}.$$

Note that this realisation is not necessarily minimal and can present unstable unobservable modes. Therefore, to simulate the process model and avoid these modes, the process is represented by the minimal realisation of (6):

$$\begin{cases} \dot{\check{x}}(t) = \check{A}\check{x}(t) + \check{B}\begin{bmatrix} u(t-L) \\ q(t-L_q) \end{bmatrix}, \\ y(t) = \check{C}\check{x}(t) + w(t), \end{cases} \tag{7}$$

where $\check{x} \in \mathbb{R}^{\check{n}}$, $\check{n}$ is the the McMillian degree of (6), the pair $(\check{A}, \check{B})$ is controllable, the pair $(\check{C}, \check{A})$ is observable and $(\check{A}, \check{B}, \check{C})$ are matrices of appropriate dimensions.

In practice, to obtain a state-space minimal realisation from a not minimal realisation, one can apply, for example, the Kalman decomposition (Kalman, 1965). Alternatively, by using MATLAB®, one can also apply the function `minreal`.

3. Simplified FSP with feedforward action

The proposed control structure is illustrated in Fig. 1. This structure combines both the SFSP to compensate dead times and a proposed feedforward structure (highlighted

in blue) to enhance the rejection of measurable disturbances. In this proposed structure, the process is represented in the upper box, $r \in \mathbb{R}$ is the set-point, whose z-transform is $R(z)$, k_r is a reference gain, K is the state feedback gain of the SFSP predictor, K_q is the state feedforward gain, k_f is the feedforward gain, $V(z)$ is the robustness filter, the signals r_s and y_s, whose z-transforms are, respectively, $R_s(z)$ and $Y_s(z)$, compose the control signal such that $u = r_s - y_s$.

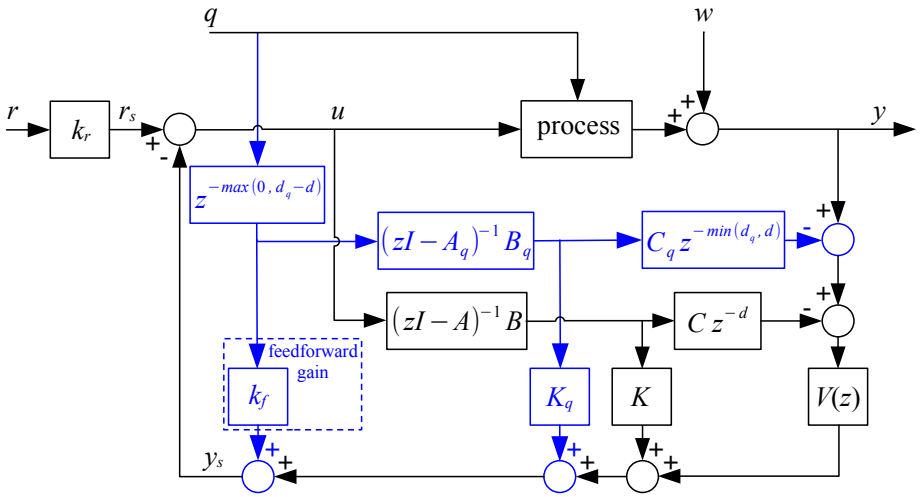

Figure 1: Conceptual proposed structure.

It is important to highlight that the proposed feedforward controller added a proportional gain k_f in the direct path, analogously to the proportional-integral (PI), to improve the transient responses of disturbance attenuation.

To better understand its design, the conceptual proposed structure can be reduced to another conceptual equivalent structure, as presented in Fig. 2, where

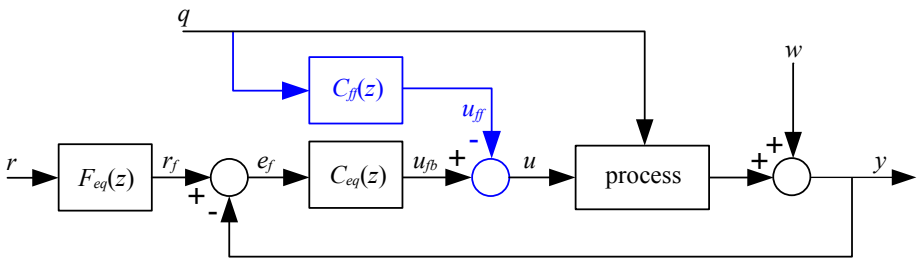

Figure 2: Conceptual equivalent structure.

$$F_{eq}(z) = \frac{R_f(z)}{R(z)} = \frac{k_r}{V(z)}, \tag{8}$$

$$C_{eq}(z) = \frac{U_{fb}(z)}{E_f(z)} = \frac{V(z)}{1 + S(z)}, \tag{9}$$

$$C_{ff}(z) = \frac{U_{ff}(z)}{Q(z)} = \frac{S_q(z)}{1 + S(z)}, \tag{10}$$

$$S(z) = \frac{\Phi(z)}{U(z)} = (K - V(z)Cz^{-d})(zI - A)^{-1}B, \tag{11}$$

$$S_q(z) = \frac{\Phi_q(z)}{Q(z)} = [k_f + (K_q - V(z)C_q z^{-\min(d_q,d)})(zI - A_q)^{-1}B_q]z^{-\max(0,d_q-d)}, \tag{12}$$

the signals r_f, e_f, u_{fb}, and u_{ff}, whose z-transforms are, respectively, $R_f(z)$, $E_f(z)$, $U_{fb}(z)$, and $U_{ff}(z)$, are defined by the relations $e_f = r_f - y$ and $u = u_{fb} - u_{ff}$.

It is important to note that, if $d \geq d_q$, (12) results

$$S_q(z) = \frac{\Phi_q(z)}{Q(z)} = k_f + (K_q - V(z)C_q z^{-d_q})(zI - A_q)^{-1}B_q \tag{13}$$

and, if $d_q > d$, it results

$$S_q(z) = \frac{\Phi_q(z)}{Q(z)} = [k_f + (K_q - V(z)C_q z^{-d})(zI - A_q)^{-1}B_q]z^{-(d_q-d)}. \tag{14}$$

As shown in Fig. 3, the signals ϕ, ϕ_q, and y_f, whose z-transforms are $\Phi(z)$, $\Phi_q(z)$ and $Y_f(z)$, compose the signal $y_s = \phi_q + \phi + y_f$. Although the conceptual structures from Figs. 1 and 2 are helpful for analysis purposes, in practice, the structure presented in Fig. 3 is used for implementation. For integrating and unstable open-loop processes, the conceptual control structure from Fig 1 is internally unstable and cannot be implemented (Torrico et al., 2021). The transfer functions $\tilde{S}(z)$ and $\tilde{S}_q(z)$, from the implementation structure, are the minimal realisations from (11) and (12), respectively.

Following the previously presented analysis, the input-output relationships of the proposed structure are given by

$$H_{yr}(z) = \frac{Y(z)}{R(z)} = k_r M(z), \tag{15}$$

$$H_{yq}(z) = \frac{Y(z)}{Q(z)} = P_q(z) - M(z)\left[k_f + K_q(zI - A_q)^{-1}B_q\right], \tag{16}$$

$$H_{uw}(z) = \frac{U(z)}{W(z)} = -V(z)\left[I - K(zI - A + BK)^{-1}B\right], \tag{17}$$

where

$$M(z) = C(zI - A + BK)^{-1}Bz^{-d}. \tag{18}$$

It is suggested to tune the proposed controller following the steps: (i) using (15) design the constant gains K and k_r for the desired closed-loop reference tracking response; (ii) design the robustness filter $V(z)$ to guarantee null steady-state error for

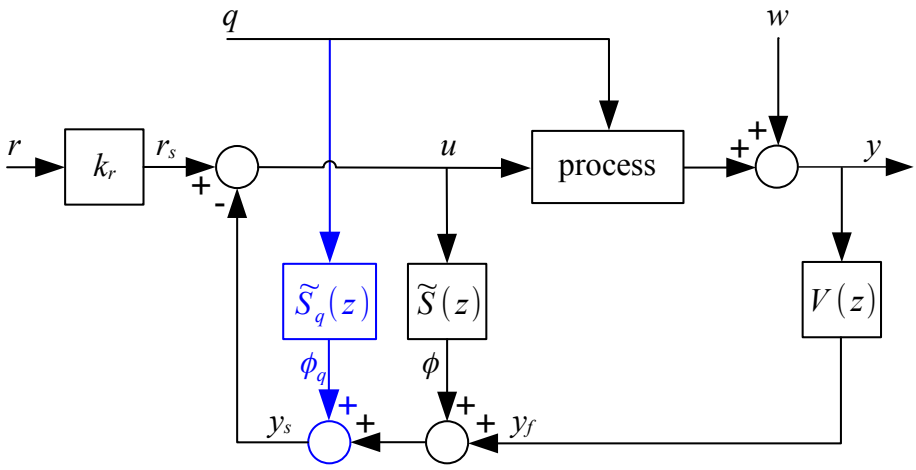

Figure 3: Implementation structure.

disturbance rejection and to satisfy the robust stability condition; (iii) using (16), design the constant gains K_q and k_f of the feedforward controller to eliminate the effects of the process model open-loop poles over the disturbance rejection response.

Alternatively, the proposed controller can be simultaneously tuned using, for example, an optimization method as in Sá Rodrigues et al. (2021). In the next section, the controller tuning is analysed in detail.

4. Controller tuning

4.1. Tuning of K and k_r

The feedback controller K is a gain vector with dimension $1 \times n$, where n is the order of the process model. It is tuned to obtain a desired characteristic polynomial

$$E_c(z) = (z - \alpha)^n = \det(zI - A + BK), \tag{19}$$

where α are the desired closed-loop poles. The pole allocation problem can be solved employing the Ackermann's formula (Ackermann, 1977):

$$K = \begin{bmatrix} 0 & 0 & \cdots & 1 \end{bmatrix} \begin{bmatrix} B & AB & \cdots & A^{n-1}B \end{bmatrix}^{-1} E_c(A). \tag{20}$$

To guarantee that (8) has unit static gain at the steady state ($z = 1$), a scalar constant gain k_r is used. Its value is computed as

$$k_r = [C(I - A + BK)^{-1}B]^{-1}, \tag{21}$$

or, alternatively,

$$k_r = \frac{1}{M(1)}, \tag{22}$$

where M is defined in (18).

4.2. Tuning of V(z)

The robustness filter $V(z)$ is designed following two objectives: (i) reject disturbances (step-like, ramp-like, sinusoidal, etc) at the steady state and (ii) cancel slow or unstable poles from the process and disturbance models. Based on these two objectives, a set of equations is defined:

$$\begin{cases} \frac{d^k}{dz^k}(1+S(z))\Big|_{z=1} = 0, k = 0, \cdots, m-1 \\ 1+S(z)\Big|_{z=p_i \neq 1} = 0, \\ 1+S(z)\Big|_{z=e^{\pm j\omega_k}} = 0, \end{cases} \tag{23}$$

where the operator $\frac{d^k}{dz^k}(\cdot)$ is the k-th derivative of $(\cdot)$ with relation to z, $m = m_1 + m_2$, m_1 is the number of poles in the model at $z = 1$, m_2 is the order of disturbance (1 for step-like, 2 for ramp-like, etc), p_i are the non-integrating undesired poles of the process and disturbance models, and ω_k are the frequencies of the sinusoidal disturbances.

The robustness filter is then defined as follows

$$V(z) = \frac{v_1 + v_2 z^{-1} + \cdots + v_{n_s} z^{-(n_s-1)}}{(1-\beta z^{-1})^{n_v}}, \tag{24}$$

where n_s is equal to the number of equations from the set (23), the number of poles are $n_v = n_s$, and β are tuning parameters which must be different from the poles of $G(z)$.

After the choice of β, using (23) and (24), a system of linear equations involving the variables v_i can be readily solved (Torrico et al., 2021).

Furthermore, from the first set of equations of (23), it can be obtained that the equivalent feedback controller $C_{eq}(z)$ has at least one pole at $z = 1$ and that $V(1) = k_r$. Therefore, the equivalent reference filter in (8) has unity static gain, that is, $F_{eq}(1) = 1$. Due to that and the integral action in $C_{eq}(z)$, any model mismatch does not result in steady-state error.

4.3. Tuning of K_q and k_f

The gains K_q and k_f must be computed following two objectives: (i) to cancel the effects of the disturbance model open-loop dynamics, improving the transient response of the disturbance rejection and (ii) to obtain an internally stable feedforward controller. Therefore, considering $S_q(z) = N_{Sq}(z)/D_{Sq}(z)$, the following conditions must be obeyed:

$$\begin{cases} \frac{d^k}{dz^k} N_{Sq}(z)\Big|_{z=1} = 0, \ k = 0, ..., \ m_q, \\ N_{Sq}(z)\Big|_{z=p_{qi} \neq 1} = 0, \end{cases} \tag{25}$$

where $m_q = m_{q1} + m_{q2}$, m_{q1} is the number of poles of $G_q(z)$ at $z = 1$, m_{q2} is the order of disturbance (1 for step-like, 2 for ramp-like, etc), and p_{qi} are the non-integrating poles of $G_q(z)$.

5. Stable implementation

Satisfying conditions (23) and (25), the proposed controller is designed to cancel the open-loop poles of the model, given by $\det(zI - A)$ and $\det(zI - A_q)$, from $S(z)$ and $S_q(z)$, respectively. Then, the canceled modes are unobservable and can lead to internal stability problems in the case of open-loop unstable or integrating processes. For practical implementation, the unobservable modes of $S(z)$ and $S_q(z)$ can be eliminated by using the minimal realizations of these transfer functions. Following the formulation from Torrico et al. (2021), expression (11) for $S(z)$ has the minimal realization

$$\tilde{S}(z) = \sum_{i=1}^{d} KA^{i-1}Bz^{-i} - \frac{N_V^*(z)}{D_V(z)}z^{-d}, \tag{26}$$

where $D_V(z)$ is the denominator of $V(z)$ and the numerator $N_V^*(z)$ is obtained by partial fraction decomposition of $G(z)V(z)$, resulting

$$G(z)V(z) = \frac{N_G^*(z)}{D_G(z)} + \frac{N_V^*(z)}{D_V(z)}. \tag{27}$$

Note that, as explained in Section 4.2, the tuning parameters β of $V(z)$ must be different from the poles of $G(z)$, guaranteeing that the partial fraction decomposition (27) is unique.

Following the formulation to obtain $\tilde{S}(z)$ from Torrico et al. (2021), the minimal realization of $S_q(z)$ is obtained, for $d \geq d_q$, as

$$\tilde{S}_q(z) = k_f + \sum_{i=1}^{d_q} K_q A_q^{i-1} B_q z^{-i} - \frac{N_{Vq}^*(z)}{D_V(z)}z^{-d_q} \tag{28}$$

and, for $d_q > d$, as

$$\tilde{S}_q(z) = \left(k_f + \sum_{i=1}^{d} K_q A_q^{i-1} B_q z^{-i} - \frac{N_{Vq}^*(z)}{D_V(z)}z^{-d}\right) z^{-(d_q-d)}, \tag{29}$$

where the partial fraction decomposition of $G_q(z)V(z)$ results as

$$G_q(z)V(z) = \frac{N_{Gq}^*(z)}{D_{Gq}(z)} + \frac{N_{Vq}^*(z)}{D_V(z)}. \tag{30}$$

It is important to note that, as explained in Section 2, the unstable poles of $G_q(z)$ are also poles of $G(z)$, guaranteeing that the partial fraction decomposition (30) is also unique.

6. Robustness analysis

Consider a dead-time process that can be modeled by unstructured multiplicative uncertainty (Morari and Zafiriou, 1989):

$$P_i(z) = P(z)(1 + \delta P_i(z)), \tag{31}$$

where $P_i(z)$ represents the process for a certain operating point within a desired region, $P(z)$ is the nominal model, and $\delta P_i(z)$ is the multiplicative uncertainty for a certain operating point.

The upper bound of the norm of the multiplicative uncertainty is computed by

$$\overline{\delta P}(\omega) \geq |\delta P_i(e^{j\Omega})| = \left| \frac{P_i(e^{j\Omega}) - P(e^{j\Omega})}{P(e^{j\Omega})} \right|, \forall i \tag{32}$$

where $\Omega = \omega T_s$, T_s is the sampling time, and ω is the frequency in the range $0 < \omega < \pi/T_s$.

Following the general robust stability theorem (Morari and Zafiriou, 1989), derived from Nyquist's stability criterion, the robust stability condition can be obtained from

$$I_r(\omega) = \frac{|1 + C_{eq}(e^{j\Omega})P(e^{j\Omega})|}{|C_{eq}(e^{j\Omega})P(e^{j\Omega})|} > \overline{\delta P}(\omega), \tag{33}$$

where $I_r(\omega)$ is the robustness index.

For the proposed structure, robust stability in the case of modeling uncertainties can be established by

$$I_r(\omega) = \left| [V(e^{j\Omega})C(e^{j\Omega}I - A)^{-1}B]^{-1}[1 + K(e^{j\Omega}I - A)^{-1}B] \right| > \overline{\delta P}(\omega). \tag{34}$$

7. Controller tuning guidelines

The main objective of tuning the SFSP with feedforward action is disturbance rejection. Although the disturbance rejection is influenced by both feedback and feedforward loops, the feedforward loop does not have free tuning parameters, and the proposed controller is tuned in the same way as the original SFSP.

The free tuning parameters of the SFSP are the closed-loop poles α, which influence both reference tracking and disturbance rejection, and the poles of the robustness filter β, which only influence the disturbance rejection. The poles α and β can be chosen between the interval $[0,\ 1)$. Their choice is made in order to meet the performance and robustness criteria of the closed-loop system. Thus, when they tend to 0, a more aggressive response will be obtained, and when they tend to 1, more robustness will be obtained.

As an illustration example, Fig. 4 shows the influence of the tuning of the poles of the robustness filter, given by β, over the robust stability condition (34). From this Figure, to satisfy condition (34) and maintain the same minimum distance between the robustness and uncertainties curves, it is easy to note that the values of β must be chosen considering the value of the dead-time uncertainty.

More information on how to properly choose the poles β of the robustness filter $V(z)$ can be found in Torrico et al. (2018); Sá Rodrigues et al. (2021).

8. Simulation examples

In this section, three simulation examples for stable, unstable, and integrating processes, where $d > d_q$, are presented. The proposed controller is compared with other

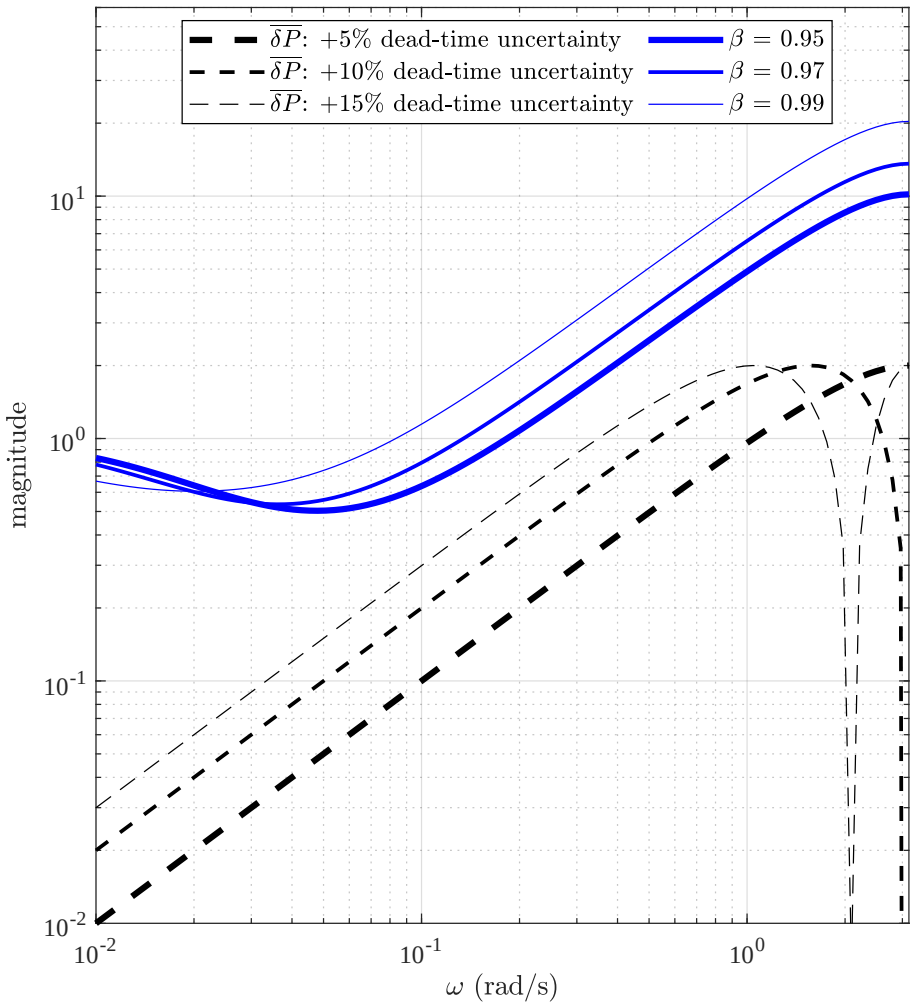

Figure 4: Robust stability for different values of dead-time uncertainties and β.

control structures from the recent literature. Only second-order or lower models are used for comparative reasons with the proposed ones found in the literature. However, the proposed controller can be applied to high-order dead-time processes by using the simple tuning strategy presented in the paper. This comparison was made taking into account the disturbance rejection performance indices, such as integrated absolute error (IAE), total variation of the control signal (TV), and control variance (CV). The expressions for these indices are

$$IAE = \int_{L}^{\infty} |r(t) - y(t)|dt, \tag{35}$$

$$TV = \sum_{i=1}^{N} |u_{i+1} - u_i|, \tag{36}$$

$$CV = \frac{1}{N-1} \sum_{i=1}^{N} |u_i - \mu|^2, \tag{37}$$

where L is the continuous-time input delay, μ and N are, the mean of the control signal and the number of samples, respectively. The CV index is computed at the beginning of the simulations when the closed-loop system is at the steady state and at the time interval when band-limited white noise is added to the output. The IAE and the TV indices are then computed only after the noise stops affecting the output.

All three simulation examples were performed using linearised models of the described processes. By using the input-output transfer functions $P(s)$ and $P_q(s)$ presented in each example and following the ideas from Section 2, the transfer functions (2) and (3), $P(z)$ and $P_q(z)$, respectively, and the state-space minimal realisation process (7) were obtained. Note that (2) and (3) were obtained by considering a zero-order hold (ZOH), while (7) was obtained using the command `minreal` from MATLAB®.

8.1. Example 1: stable process

The model of a boiler is used to assess the performance of the proposed strategy. The process is from the Abbott Power Plant in Champaign, IL, which is powered by oil and gas and used for heating and power generation (Pellegrinetti and Bentsman, 1996). It is desired to control the steam pressure $y_1(t)$, while the fuel rate $u_1(t)$ is the manipulated variable and the steam demand $d_1(t)$ is the measurable disturbance. Other inputs, outputs, and disturbances are considered constant, as in Pellegrinetti and Bentsman (1996). Hence, one can find the linearized process and disturbance transfer functions of the boiler, respectively, as

$$P(s) = \frac{0.355}{24.75s + 1} e^{-6.75s}, \tag{38}$$

$$P_q(s) = \frac{-0.712}{195.8s + 1}. \tag{39}$$

The equivalent discrete-time transfer functions with sampling period $T_s = 0.25$ s are

$$P(z) = \frac{0.003568}{z - 0.9899} z^{-27}, \tag{40}$$

$$P_q(z) = \frac{-0.0009085}{z - 0.9987}. \tag{41}$$

The controller was designed to compute the feedback gain K in order to obtain a closed-loop pole $\alpha = 0.75$ and the robustness filter was designed with poles $\beta = 0.988$ with multiplicity $n_v = 3$, to satisfy the robustness condition (34) for a dead-time uncertainty of 10% in the process model and to attenuate the measurement noise.

A comparison of the proposed controller (SFSP-FF) is made with those presented in Alves Lima et al. (2019) and Rodríguez et al. (2016). All these controllers have feedforward action for measurable disturbances. The controller from Rodríguez et al. (2016) was tuned in the continuous-time domain, for set-point tracking, with $\tau_{rt} = 6.75$ and, for disturbance rejection, with $\tau_{sp} = 20$ and $\tau_{dr} = 1.5$. The controller from Alves Lima et al. (2019) was tuned in the discrete-time domain, for set-point tracking, with $p_c = 0.5724$, for disturbance rejection, with $\beta_{SDTC-FF} = 0.9752$ and $\alpha_{SDTC-FF} = 0.8796$. As the SFSP-FF, these two controllers were implemented in the discrete-time domain with sampling period $T_s = 0.25\ s$. The components of the controllers being compared are shown in Table 1.

Table 1: Example 1 - Controllers parameters.

	Rodríguez et al. (2016)	Alves Lima et al. (2019)	SFSP-FF
Reference filter	$\frac{0.01815}{z-0.9818}$	119.8401	67.2541
Feedback controller	$\frac{10.33z-10.22}{z-1}$	117.0232	70.0710
Robustness filter	$\frac{0.7308z^2-1.431z+0.6999}{(z-0.9876)^2}$	$\frac{2.974z}{z-0.9752}$	$\frac{2.018z^3-4.003z^2+1.985z}{(z-0.988)^3}$
k_f	-	-	-1.9366
K_q	-	-	67.3510
Feedforward filter	$\frac{28.57z^2-55.24z+26.69}{(z-0.8465)^2}$	$\frac{531.1z-516.6}{z-0.8796}$	-

Figure 5 shows the robustness condition from (34) considering the given process model uncertainty. For a fair comparison, all controllers have similar robustness. Figures 6 and 7 show the output and control signals for the simulations of the nominal case and of the case with model uncertainties, respectively. In the simulation, white noise of power $5 \cdot 10^{-4}$ was added to the process output at the first 10 s, a step disturbance of $d_1(t) = 30\%$ in the steam demand occurs at $t = 20\ s$. Even though all the compared controllers have been designed with similar levels of robustness, the proposed controller rejects the disturbance much faster, as confirmed by the IAE indices shown in Table 4. Because of the more aggressive response, as expected, the TV index of the proposed controller is higher.

8.2. Example 2: unstable process

In this example, the control of a chemical reactor with a non-ideal mixture is studied. Its nonlinear model is described by

$$\frac{\mathrm{dC(t)}}{\mathrm{d}t} = \frac{F(t)}{V}[C_i(t) - C(t)] - \frac{k_1 C(t)}{[k_2 C(t) + 1]^2} \tag{42}$$

where $C_i(t)$ and $C(t)$ are the input and output concentrations, respectively, $F(t)$ is the inflow and V is the reactor volume. The values of the constant parameters of the model are $k_1 = 10\ l/s$, $k_2 = 10\ l/mol$, and $V = 1\ l$.

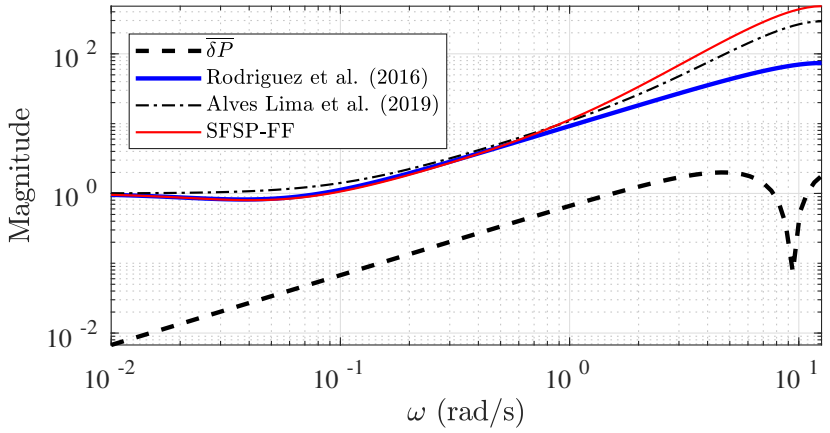

Figure 5: Example 1. Robustness index.

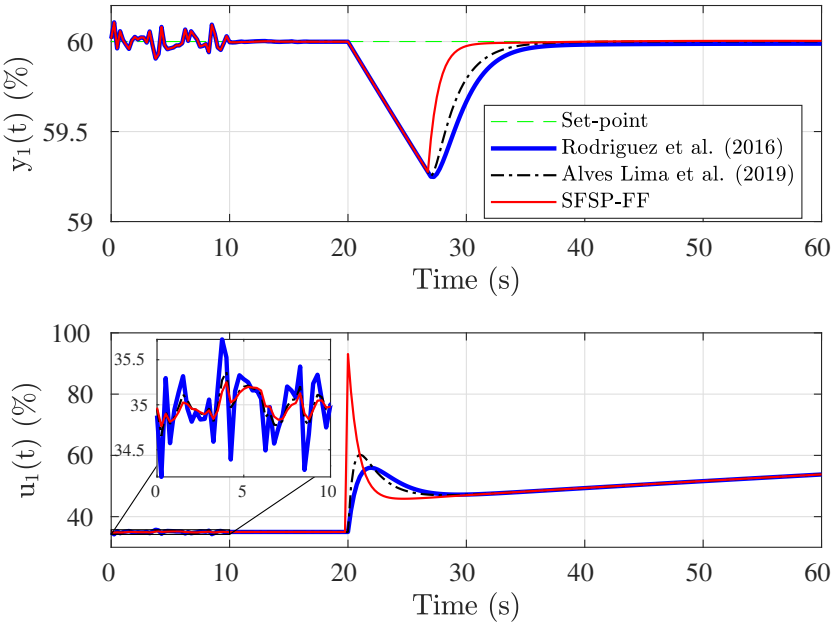

Figure 6: Example 1. Nominal case.

For control purposes, as studied in Chidambaram and Reddy (1996), $C(t)$ is the variable to be controlled, $C_i(t)$ is the manipulated variable, and $F(t)$ is the disturbance variable. The linearised model at its operation point has the following transfer functions (Rodríguez et al., 2016):

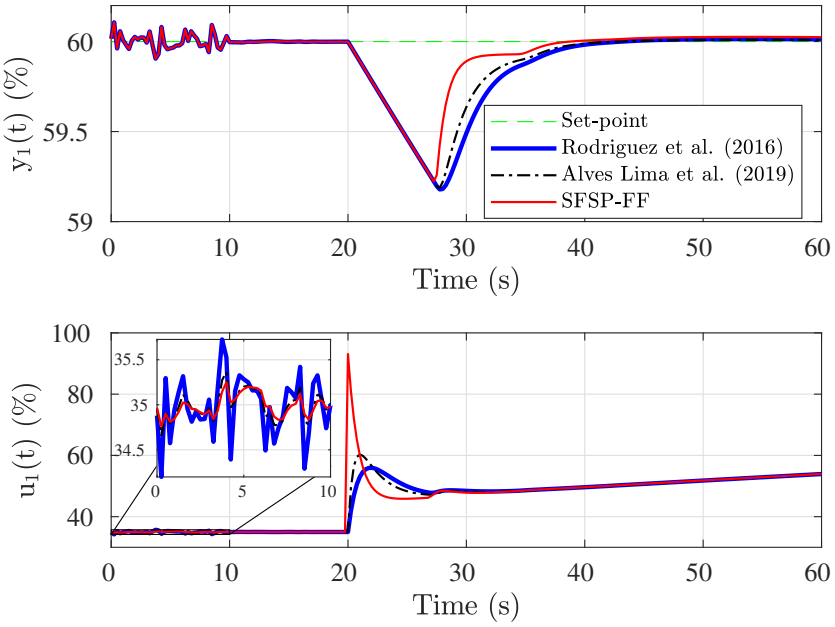

Figure 7: Example 1. Case with model uncertainties.

$$P(s) = \frac{3.433}{103.1s - 1} e^{-20s}, \tag{43}$$

$$P_q(s) = \frac{-206.9346}{103.1s - 1} e^{-10s}. \tag{44}$$

Discretisation of the transfer functions with sampling period $T_s = 1\ s$, leads to:

$$P(z) = \frac{0.03364}{z - 1.01} z^{-20}, \tag{45}$$

$$P_q(z) = \frac{-2.017}{z - 1.01} z^{-10}. \tag{46}$$

In this example, two different tunings of the SFSP-FF are considered, namely SFSP-FF1 and SFSP-FF2. For the SFSP-FF1, the feedback controller was tuned with $\alpha = 0.2$, while for the SFSP-FF2, it was chosen $\alpha = 0.7$. As $P(z)$ is a first-order transfer function, for both tunings, $n = 1$. To satisfy the robustness condition (34) for a dead-time uncertainty of 10% in the process model and to attenuate measurement noise, for both controllers, the robustness filter was tuned with $\beta = 0.98$ with multiplicity $n_v = 2$. Both controllers are compared with the one presented in Rodríguez et al. (2016), that was tuned, for set-point tracking, with $\tau_{rt} = 20$, for disturbance rejection, with $\tau_{sp} = 26$ and $\tau_{dr} = 2.5$. As the proposed controllers, the one from Rodríguez et al. (2016) was

Table 2: Example 2 - Controllers parameters.

	Rodríguez et al. (2016)	SFSP-FF1	SFSP-FF2
Reference filter	$\frac{0.4558z-0.4333}{(z-0.9775)}$	23.9093	8.9660
Feedback controller	$\frac{3.294z-3.219}{z-1}$	24.2006	9.2573
Robustness filter	$\frac{1.256z^3-3.632z^2+3.5z-1.124}{(z-0.9623)^2}$	$\frac{1.66z^2-1.651z}{(z-0.98)^2}$	$\frac{0.6425z^2-0.639z}{(z-0.98)^2}$
k_f	-	-570.3513	-255.3927
K_q	-	26.6655	10.2002
Feedforward filter	$\frac{23.45z^3-66.13z^2+62.09z-19.41}{(z-0.6703)^2}$	-	-

implemented in the discrete-time with sampling period $T_s = 1\ s$. The components of the three controllers are presented in Table 2.

Figure 8 shows the robustness indices of the controllers being compared considering the dead-time uncertainty. As can be seen, the robustness of the two tunings of the SFSP-FF is better at medium and high frequencies, where the robust stability condition is critical when considering dead-time uncertainties (Normey-Rico and Camacho, 2007).

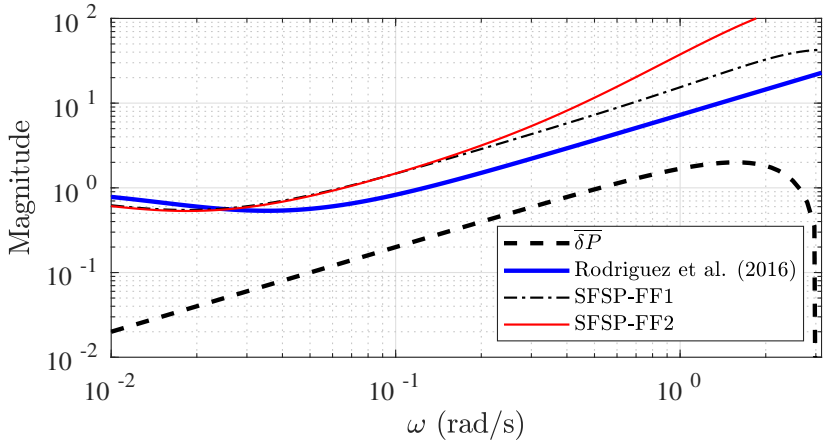

Figure 8: Example 2. Robustness Index.

For simulation, white noise with power of $1 \cdot 10^{-3}$ is added to the output at the first 50 s and a disturbance of $F(t) = 0.015l/s$ is applied to the input flow at $t = 100\ s$. The time responses of the controllers for the nominal case and the case with model uncertainties are shown in Figs. 9 and 10, respectively. From these figures, it is evident that the two tunings of the proposed controllers provide faster disturbance rejection, as confirmed by the performance indices presented in Table 4. The FSFP-FF1 tuning presented the best IAE index and the highest TV index, due to the aggressiveness of the tuning. The SFSP-FF2, with a more robust tuning, presented the best TV and CV indices and a better IAE than the controller from Rodríguez et al. (2016).

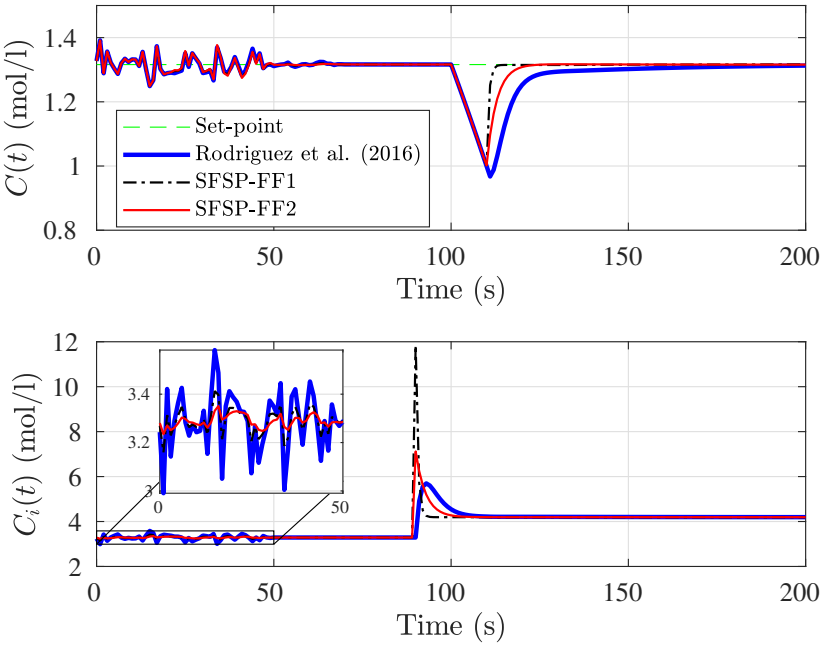

Figure 9: Example 2. Nominal case.

8.3. Example 3: integrating disturbance

In this case, a continuous stirred-tank reactor (CSTR) model is studied (Henson and Seborg, 1997). The CSTR performs an irreversible reaction where its temperature $T(t)$ is controlled with external cooling with temperature $T_c(t)$ and the disturbance is $V_0(t) = \int_0^t F_0(\tau)d\tau$, where $F_0(t)$ is the measurable inlet flow rate.

As defined in Rodríguez et al. (2016), the transfer functions for a certain operating point are given by

$$P(s) = \frac{1.7316(s + 1.178)}{(s^2 + 1.757s + 1.207)}e^{-s}, \tag{47}$$

$$P_q(s) = \frac{0.048615(s - 4.275)(s + 1.358)}{(s^2 + 1.757s + 1.207)}e^{-0.25s}. \tag{48}$$

Discretisation of the transfer functions with sampling period $T_s = 0.05$ s leads to

$$P(z) = \frac{0.085321(z - 0.9428)}{(z^2 - 1.913z + 0.9159)}z^{-20}, \tag{49}$$

$$P_q(z) = \frac{0.002148(z - 1.239)(z - 0.9343)}{(z^2 - 1.913z + 0.9159)}z^{-5}. \tag{50}$$

The SFSP-FF was tuned with desired closed-loop poles $\alpha = 0.95$ with multiplicity $n = 2$ and, for the robustness filter, with poles $\beta = 0.97$ with multiplicity $n_v = 4$.

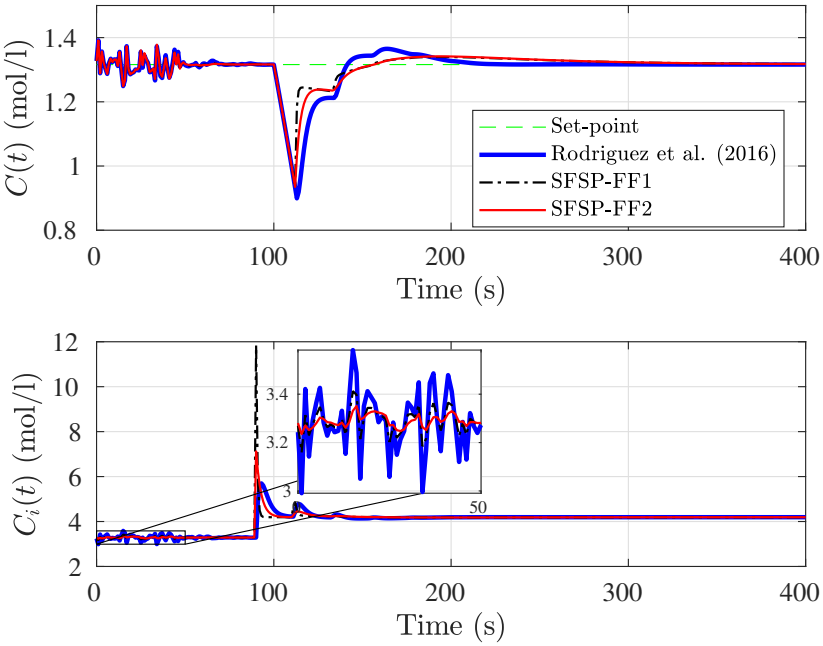

Figure 10: Example 2. Case with model uncertainties.

The proposed controller is compared with the control strategy presented by Rodríguez et al. (2016). This strategy was tuned in the continuous-time domain, for set-point tracking, with $\tau_{rt} = 10$, for disturbance rejection, with $\tau_{sp} = 1$ and $\tau_{dr} = 0.5$. It was implemented in the discrete-time domain with sampling period $T_s = 0.05\ s$. Table 3 shows the components of both controllers.

A dead-time uncertainty of 10% is considered in the case with model uncertainties. The robustness indices of both controllers are shown in Fig. 11. The proposed controller presents a better index at medium and high frequencies.

In the simulation, white noise of power $5 \cdot 10^{-4}$ is added to the output for the first $t = 5\ s$ and a disturbance of $F_0(t) = 20\ l/min$ in the inlet flow rate is applied at $t = 10\ s$, which is equivalent to apply a ramp-like disturbance $V_0(t) = 20(t-10)\ (l)$ to the process. Figures 12 and 13 show the time responses for the nominal case and the case with model uncertainties, respectively. The proposed controller presents faster disturbance rejection with a smaller undershoot. Table 4 shows that the SFSP-FF presented better indices in all compared scenarios. It is worth noting that the IAE and CV are much smaller than those of the controller from (Rodríguez et al., 2016).

Table 3: Example 3 - Controllers parameters.

	Rodríguez et al. (2016)	SFSP-FF
Reference filter	$\frac{0.05719}{(z-0.9428)}$	0.5123
Feedback controller	$\frac{1.208z^2-2.528z+1.322)}{(z-1)(z-0.946)}$	[10.7204 11.2087]
Robustness filter	$\frac{1.649z^2-3.263z+1.614}{(z-0.9512)^2}$	$\frac{0.01861z^4-0.05394z^3+0.05213z^2-0.0168z}{(z-0.97)^4}$
k_f	-	-0.0699
K_q	-	[140.8091 136.0207 130.9232]
Feedforward filter	$\frac{3.682z^2-7.242z+3.56}{(z-0.9048)^2}$	-

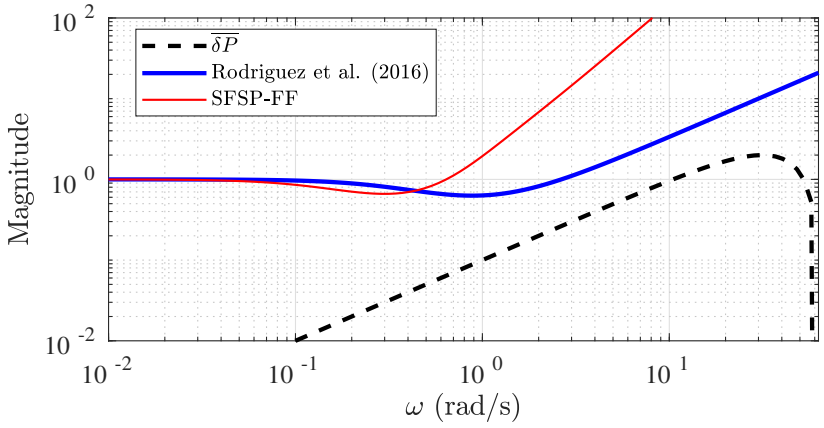

Figure 11: Example 3. Robustness Index.

9. Temperature control in a NICU

Experiments in a NICU were performed to evaluate the proposed strategy in a practical application. Figure 14 shows a picture of the NICU connected to a desktop computer. This computer can communicate with the NICU's hardware to receive the internal temperature and relative humidity measurements and send the pulse width modulation (PWM) duty cycles of the voltages at the heater and humidifier. Therefore, the complete system of the NICU is a two-inputs-two-outputs process. However, only the temperature loop is of interest in the performed experiments.

The process variable is the temperature in the NICU and the control variable is the PWM duty cycle of the voltage at the heater. Disturbances occur when the ports of the NICU are opened and the external cooler air goes into the NICU's dome. Therefore, in these experiments, a unit step change in the measurable disturbance input is considered when one port is opened.

By performing an identification experiment, the following discrete-time transfer functions, with sampling period $T_s = 0.4$ min, were obtained

$$P(z) = \frac{0.002718}{z - 0.9621} z^{-6}, \tag{51}$$

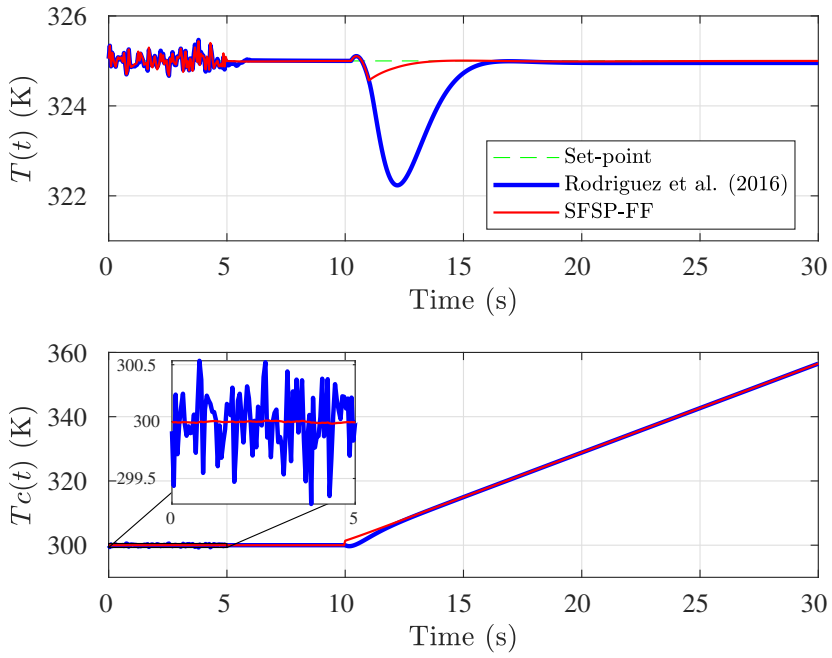

Figure 12: Example 3. Nominal case.

$$P_q(z) = \frac{-0.06204}{z - 0.9445} z^{-30}. \tag{52}$$

Note in (51) and (52) that $d_q > d$. Therefore, the tuning of the proposed controller is based on the appropriate formulation for this case.

The SFSP-FF is compared to the SFSP presented in Torrico et al. (2021). The two controllers were tuned for set-point tracking with $\alpha = 0.85$ with multiplicity $n = 1$. The robustness filters of both controllers were tuned to satisfy condition (34), considering the uncertainties of $P(z)$ as +10% in the static gain and time constant, and +0.4 min in the dead time. After a considerable number of model identification procedures, at different operation points, it was observed that each of the model parameters varied up to a certain range. Therefore, the considered uncertainty for each parameter follow this range. The upper bound of the norm of multiplicative uncertainty, computed by (32), results

$$\overline{\delta P}(\omega) = \left| \frac{1 - 0.962 e^{-j\omega T_s}}{e^{j\omega T_s} - 0.9654} - 1 \right|. \tag{53}$$

The SFSP was tuned with $\beta = 0.85$ with multiplicity $n_v = 2$, while the SFSP-FF was tuned with $\beta = 0.9$ with multiplicity $n_v = 3$. The parameters of both controllers are presented in Table 5.

The robustness indices of both controllers are presented in Fig. 15, where it can be seen that the proposed strategy presents better index at mid and high frequencies.

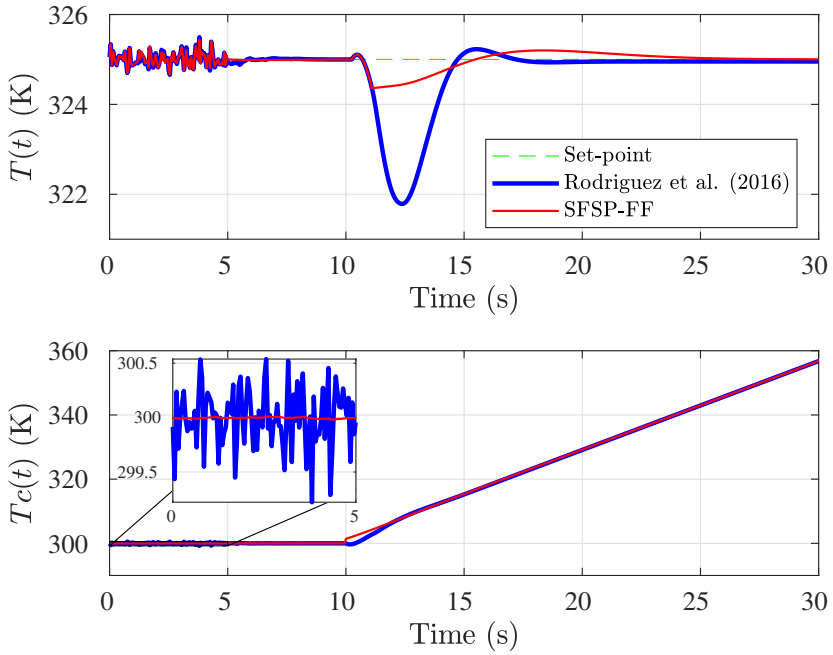

Figure 13: Example 3. Case with model uncertainties.

Figure 16 shows the temperature responses from the NICU for both controllers. A set-point step change from 24^{o}C to 28^{o}C was applied at t = 10 min and one port of the NICU was opened at t = 58 min. For the SFSP-FF, the unit step change in the measurable disturbance input was also applied at t = 58 min. From Fig. 16, it can be seen that the control input of the SFSP-FF begins to actuate sooner than the control input of the SFSP to reject the disturbance. This results in a much faster disturbance rejection by the SFSP-FF than by the SFSP.

Table 6 shows the IAE index for both controllers, computed in the time interval while the port of the NICU is open. The IAE was calculated by

$$IAE = \int_0^\infty |r(t) - y(t)|dt. \tag{54}$$

Note that the IAE of the SFSP-FF is 40.23% smaller than the IAE of the SFSP.

10. Conclusions

This work presented a feedforward controller for a strategy based on the Smith predictor. When dealing with measurable disturbances, the proposed controller has faster disturbance rejection when compared to other controllers from the recent literature. Furthermore, this is accomplished by maintaining a simple control structure based on

Table 4: Performance indices. The best performances are highlighted in bold text.

Example		Nominal			Perturbed		
		IAE	TV	CV	IAE	TV	CV
Example 1	SFSP-FF	**0.76**	55.20	**0.015**	**2.21**	56.67	**0.015**
	Alves Lima et al. (2019)	2.00	45.34	0.025	3.57	46.00	0.025
	Rodríguez et al. (2016)	2.96	**36.28**	0.11	4.13	**36.03**	0.11
Example 2	SFSP-FF1	**0.29**	7.66	0.0027	**5.70**	9.19	0.0028
	SFSP-FF2	0.89	**2.93**	**0.0006**	6.58	**3.48**	**0.0006**
	Rodríguez et al. (2016)	3.11	3.91	0.015	7.09	5.50	0.016
Example 3	SFSP-FF	**0.50**	**55.14**	**0.00003**	**2.95**	**55.41**	**0.00003**
	Rodríguez et al. (2016)	6.48	57.14	0.065	7.28	57.42	0.07

Figure 14: Temperature control in a NICU connected to a desktop computer.

Table 5: Temperature control in a NICU - Controllers parameters.

	Torrico et al. (2021)	SFSP-FF
Reference gain	55.1861	55.1861
Feedback controller	41.2255	41.2255
Robustness filter	$\frac{21.48z^2-20.24z}{(z-0.85)^2}$	$\frac{16.37z^3-30.89z^2+14.57z}{(z-0.9)^3}$
k_f	-	-22.8247
K_q	-	34.7522

Temperature control in a NICU	IAE
SFSP-FF	**5.78**
Torrico et al. (2021)	9.67

Table 6: IAE index for disturbance rejection. The best index is highlighted in bold text.

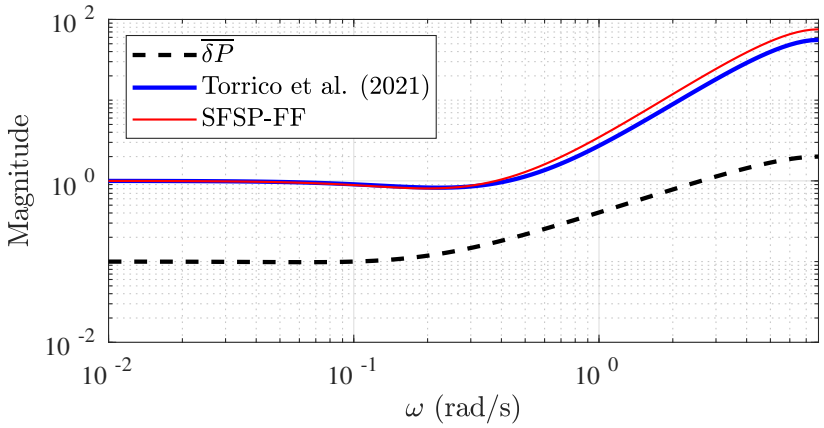

Figure 15: Temperature control in a NICU. Robustness index.

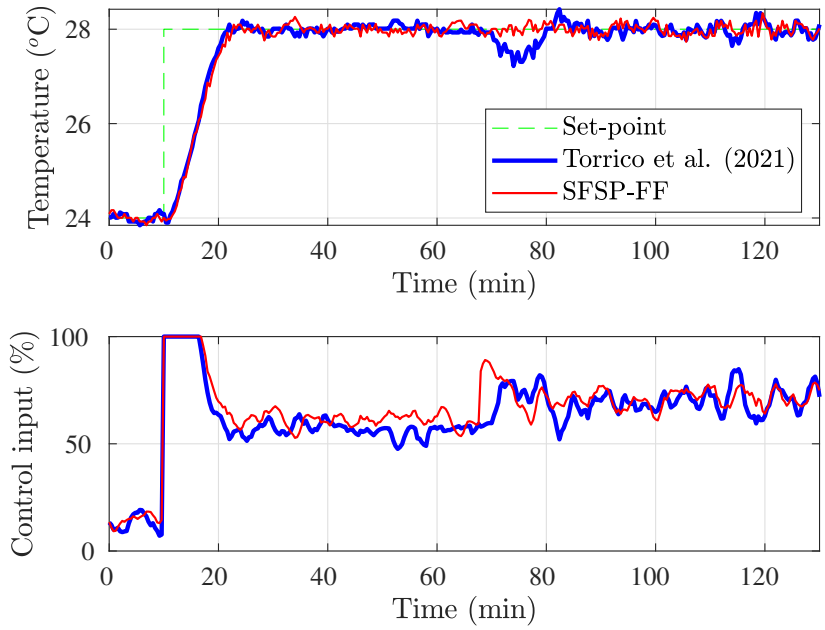

Figure 16: Temperature control in a NICU. Temperature responses from the NICU.

just two free tuning parameters, the feedback gain K and the robustness filter $V(z)$, while the controllers being compared with present one more free tuning parameter, the feedforward filter.

From simulation results, the proposed controller showed better IAE and CV indices

for all six scenarios. The improvement in the IAE index was between 61, 5% to 1196%, even with similar or better robustness. Even though enhanced performance for disturbance rejection was achieved, the TV index was better in four out of six scenarios, thus showing a good compromise between performance and robustness.

In the temperature control in a NICU, a real application, the proposed strategy showed better results than the conventional SFSP, with faster disturbance rejection response and improving in 40.23% the IAE index. Furthermore, this application is a versatile example of how the proposed feedforward control system can be implemented in practice.

Therefore, given its effectiveness and promising results, the proposed controller shows great potential for real industrial applications.

Appendix A. Observable canonical form

A process model with dead time $T(z) = X(z)z^{-h}$ can be represented as

$$T(z) = \frac{b_n z^{n-1} + b_{n-1} z^{n-2} + \cdots + b_2 z + b_1}{z^n + a_n z^{n-1} + \cdots + a_2 z + a_1} z^{-h} = C(zI - A)^{-1} B z^{-h}, \tag{55}$$

where, in the canonical observable form,

$$A = \begin{bmatrix} -a_n & 1 & 0 & \cdots & 0 \\ -a_{n-1} & 0 & 1 & \cdots & 0 \\ \vdots & \vdots & \vdots & \ddots & 0 \\ -a_2 & 0 & 0 & \cdots & 1 \\ -a_1 & 0 & 0 & \cdots & 0 \end{bmatrix}_{n\times n}, \; B = \begin{bmatrix} b_n \\ b_{n-1} \\ \vdots \\ b_2 \\ b_1 \end{bmatrix}_{n\times 1}, \; C = \begin{bmatrix} 1 & 0 & \cdots & 0 \end{bmatrix}_{1\times n}. \tag{56}$$

Acknowledgements

Financial support from the Brazilian funding agencies CAPES (Brazil), CNPq (Brazil) [Grant Number 313000/2021-2, CNPq 18/2021 - Grant Number 422633/2021-6], and FUNCAP (Brazil) [FUNCAP No 06/2021 - Grant Number 09779122/2021] is gratefully acknowledged.

References

Ackermann, J.E., 1977. On the synthesis of linear control systems with specified characteristics. Automatica 13, 89 – 94.

Albertos, P., García, P., 2009. Robust control design for long time-delay systems. Journal of Process Control 19, 1640–1648.

Albertos, P., Sanz, R., Garcia, P., 2015. Disturbance rejection: A central issue in process control, in: 2015 4th International Conference on Systems and Control (ICSC), pp. 1–8.

Alves Lima, T., Torrico, B.C., De Almeida Filho, M.P., Forte, M.D.N., Pereira, R.D.O., Nogueira, F.G., 2019. First-order dead-time compensation with feedforward action, in: 2019 18th European Control Conference (ECC), pp. 3638–3643.

Castillo, A., García, P., 2021. Predicting the future state of disturbed LTI systems: A solution based on high-order observers. Automatica 124, 109365.

Castillo, A., García, P., Fridman, E., Albertos, P., 2019. Extended state observer-based control for systems with locally Lipschitz uncertainties: LMI-based stability conditions. Systems & Control Letters 134, 104526.

Chen, C.T., 1984. Linear system theory and design. Saunders college publishing.

Chidambaram, M., Reddy, G.P., 1996. Nonlinear control of systems with input and output multiplicities. Computers & Chemical Engineering 20, 295–299.

Davison, E.J., 1973. The feedforward control of linear multivariable time-invariant systems. Automatica 9, 561–573.

García, P., Albertos, P., 2013. Robust tuning of a generalized predictor-based controller for integrating and unstable systems with long time-delay. Journal of Process Control 23, 1205–1216.

García-Mañas, F., Guzmán, J.L., Rodríguez, F., Berenguel, M., Hägglund, T., 2021. Experimental evaluation of feedforward tuning rules. Control Engineering Practice 114, 104877.

Geng, X., Hao, S., Liu, T., Zhong, C., 2019. Generalized predictor based active disturbance rejection control for non-minimum phase systems. ISA Transactions 87, 34 – 45.

Guzmán, J.L., Hägglund, T., 2011. Simple tuning rules for feedforward compensators. Journal of Process Control 21, 92–102.

Hast, M., Hägglund, T., 2014. Low-order feedforward controllers: Optimal performance and practical considerations. Journal of Process Control 24, 1462–1471.

Henson, M.A., Seborg, D.E., 1997. Nonlinear process control. Prentice Hall PTR Upper Saddle River, New Jersey.

Kalman, R.E., 1965. Irreducible realizations and the degree of a rational matrix. Journal of the Society for Industrial and Applied Mathematics 13, 520–544.

Liu, T., García, P., Chen, Y., Ren, X., Albertos, P., Sanz, R., 2018. New predictor and 2DOF control scheme for industrial processes with long time delay. IEEE Transactions on Industrial Electronics 65, 4247–4256.

Liu, T., Hao, S., Li, D., Chen, W.H., Wang, Q.G., 2019. Predictor-based disturbance rejection control for sampled systems with input delay. IEEE Transactions on Control Systems Technology 27, 772–780.

Morari, M., Zafiriou, E., 1989. Robust process control. Prentice Hall.

Normey-Rico, J.E., Camacho, E.F., 2007. Control of dead-time processes. Springer.

Normey-Rico, J.E., Camacho, E.F., 2009. Unified approach for robust dead-time compensator design. Journal of Process Control 19, 38 – 47.

Pellegrinetti, G., Bentsman, J., 1996. Nonlinear control oriented boiler modeling – a benchmark problem for controller design. IEEE Transactions on Control Systems Technology 4, 57–64.

Rodríguez, C., Aranda-Escolástico, E., Guzmán, J.L., Berenguel, M., Hägglund, T., 2020. Revisiting the simplified internal model control tuning rules for low-order controllers: Feedforward controller. IET Control Theory and Applications 14, 1612–1618.

Rodríguez, C., Normey-Rico, J.E., Guzmán, J.L., Berenguel, M., Dormido, S., 2016. Low-order feedback-feedforward controller for dead-time processes with measurable disturbances. IFAC-PapersOnLine 49, 591–596.

Rodríguez, C., Normey-Rico, J., Guzmán, J., Berenguel, M., 2016. On the filtered Smith predictor with feedforward compensation. Journal of Process Control 41, 35 – 46.

Sanz, R., García, P., Albertos, P., 2018. A generalized Smith predictor for unstable time-delay SISO systems. ISA Transactions 72, 197 – 204.

Sanz, R., García, P., Díez, J.L., Bondia, J., 2021. Artificial pancreas system with unannounced meals based on a disturbance observer and feedforward compensation. IEEE Transactions on Control Systems Technology 29, 454–460.

Sanz, R., García, P., Fridman, E., Albertos, P., 2020. Robust predictive extended state observer for a class of nonlinear systems with time-varying input delay. International Journal of Control 93, 217–225.

Silva, W.A., Torrico, B.C., Correia, W.B., dos Reis, L.L., 2018. Adaptive feedforward control applied in switched reluctance machines drive speed control in fault situations. Journal of Dynamic Systems, Measurement, and Control 140.

Smith, O.J.M., 1957. Closer control of loops with dead time. Chemical Engineering Progress 53, 217–219.

Sá Rodrigues, R.C., Sombra, A.K.R., Torrico, B.C., Pereira, R.D.O., do N. Forte, M.D., de Almeida Filho, M.P., Nogueira, F.G., 2021. Tuning rules for unstable dead-time processes. European Journal of Control 59, 250–263.

Torrico, B.C., de Almeida Filho, M.P., Alves Lima, T., do N. Forte, M.D., Sá, R.C., Nogueira, F.G., 2018. Tuning of a dead-time compensator focusing on industrial processes. ISA Transactions 83, 189 – 198.

Torrico, B.C., Pereira, R.D.O., Sombra, A.K.R., Nogueira, F.G., 2021. Simplified filtered Smith predictor for high-order dead-time processes. ISA Transactions 109, 11–21.

Zhang, B., Tan, W., Li, J., 2020. Tuning of Smith predictor based generalized ADRC for time-delayed processes via IMC. ISA Transactions 99, 159 – 166.

Zhao, S., Gao, Z., 2014. Modified active disturbance rejection control for time-delay systems. ISA Transactions 53, 882 – 888.